MODIS reflective solar bands calibration improvements for Collection 7

Kevin Twedt,*[a] Emily Aldoretta,[a] Amit Angal,[a] Hongda Chen,[a] Xu Geng,[a] Yonghong Li,[a] Qiaozhen Mu,[a] Kevin Vermeesch,[b] and Xiaoxiong Xiong[c]

[a]Science Systems and Applications Inc., Lanham, MD 20706, USA
[b]Global Science and Technology Inc., Greenbelt, MD 20770, USA
[c]Sciences and Exploration Directorate, NASA/GSFC, Greenbelt, MD 20771, USA

ABSTRACT

Calibration of Terra and Aqua MODIS reflective solar bands (RSB) has evolved significantly since the launch of the first MODIS instrument on the Terra satellite more than 21 years ago. In NASA's current Collection 6 and 6.1 Level 1B products (C6/C6.1 L1B), the RSB calibration algorithm continues to rely primarily on the onboard solar diffuser to calibrate the instrument gain. Lunar observations are used to track on-orbit changes in the response versus scan angle (RVS), and data from pseudo-invariant desert sites are used to apply adjustments to the gain and RVS calibration for select bands. The resulting reflectance products have in general shown a very stable performance. In recent years, some performance degradation has been noted for a few bands and algorithm changes have been tested to further improve the calibration accuracy for the upcoming Collection 7 (C7) L1B reprocess. In this paper, we present the MODIS RSB calibration improvements that will be included in C7. Major improvements include: applying polarization correction to the desert data before using it to generate RVS for Terra bands 8, 9, 3, and 10; using ocean scene data and an interband calibration approach to correct for long-term drift of Terra bands 11 and 12; applying an updated crosstalk correction to Terra SWIR bands over the entire mission; and using data from deep convective clouds in Terra SWIR band calibration, including the addition of time-dependent RVS for bands 5 and 26. All other minor calibration changes are also covered. Overall, the reflectance differences at nadir between C6.1 and C7 are within a few percent, though the differences increase in some cases at large scan angles. The Terra visible (3, 8-12) and SWIR bands (5-7, 26) have the most significant improvements. For all other Terra bands and all Aqua bands, the C7-C6.1 differences are mostly within 1%.

Keywords: MODIS, reflective solar bands, solar diffuser, polarization, deep convective clouds

1. INTRODUCTION

Accurate calibration is critically important to the quality of the many Earth science products derived from NASA's MODIS instruments on board the Terra and Aqua spacecraft. Over more than two decades of operation, several different calibration algorithms have been used and several different versions, or Collections, of the Level 1B (L1B) calibrated imagery data have been released. To aid in accurate on-orbit tracking of the instrument calibration, each MODIS is equipped with several on-board calibrators (OBC). A solar diffuser (SD) is the primary calibration source for the reflective solar bands (RSB), covering the visible through short-wave infrared (SWIR) wavelengths, and a blackbody is the primary calibration source for the thermal emissive bands. A spectro-radiometric calibration assembly (SRCA) is also capable of tracking the radiometric, spatial, and spectral performance of MODIS bands.[1,2]

In NASA's current Collection 6 and 6.1 (C6/C6.1) L1B products, the RSB calibration algorithm continues to rely primarily on the onboard SD to calibrate the instrument gain. In addition, lunar observations are used to track on-orbit changes in the response versus scan angle (RVS), and data from pseudo-invariant desert sites are used to apply adjustments to the gain and RVS calibration for select bands.[3,4] In previous MODIS Collections, the SRCA was also used as part of the RSB calibration algorithm, but it is no longer used due to degradation and failures of some of the lamp sources.

The C6.1 reflectance products have in general shown very stable performance.[5,6] In recent years, some performance degradation has been noted for a few bands and algorithm changes have been tested to further improve the calibration accuracy for the upcoming Collection 7 (C7) L1B reprocess. This paper provides details of the algorithm changes made to MODIS RSB calibration for the mission-reprocessed RSB look-up-tables (LUT) to be used in C7. Figure 1 shows a list of the main algorithm changes and the bands on each instrument which are affected. Major improvements include: applying polarization correction to the desert data before using it to generate RVS for Terra bands 8, 9, 3, and 10; applying an updated crosstalk correction to Terra SWIR bands over the entire mission; using data from deep convective clouds (DCC) in Terra SWIR band calibration, including the addition of time-dependent RVS for bands 5 and 26; using ocean scene data and an interband calibration approach to correct for long-term drift of Terra bands 11 and 12; enhancements to the processing and fitting of desert data used in calibration; addition of detector-dependent RVS to Terra band 4; and using an improved screen vignetting function in SD calibration for Aqua ocean bands. All other minor calibration changes are also covered. The center wavelengths for each MODIS RSB are provided in Table 1 for reference.

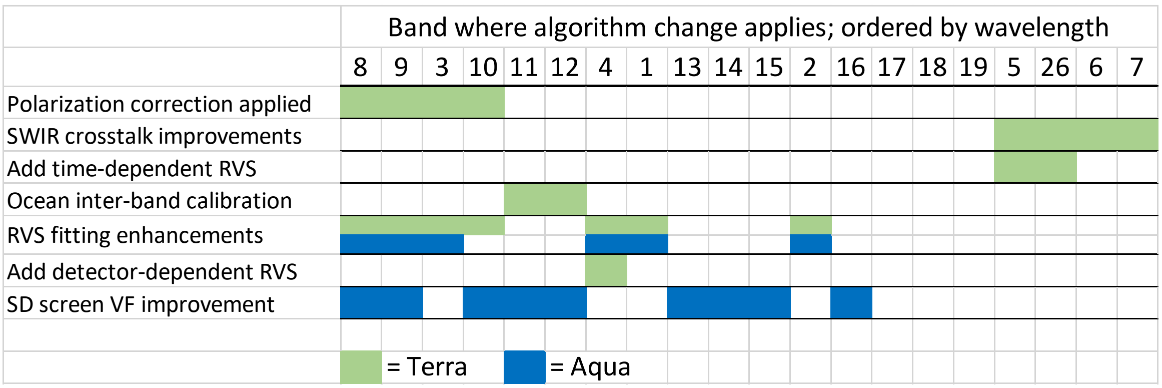

Figure 1. List of changes for C7 roughly ordered from the largest impact (top) to smallest (bottom). Colors indicate the band and instrument to which each change is applied. The MODIS bands are ordered by wavelength from shortest on the left to longest on the right.

Table 1. Center wavelengths of MOIDS reflective solar bands in nm.

Band	Wavelength	Band	Wavelength	Band	Wavelength
1	645	8	412	17	905
2	858	9	443	18	936
3	469	10	488	19	940
4	555	11	531	26	1375
5	1240	12	551		
6	1640	13	667		
7	2130	14	678		
		15	748		
		16	869		

The current C6.1 algorithms are reviewed briefly in Section 2, the algorithm changes made for C7 relative to C6.1 are discussed in Section 3, and the impacts on the final C7 L1B reflectance product are shown in Section 4. The changes to the corresponding RSB uncertainty index are discussed briefly in Section 5. The initial mission-reprocessed RSB LUTs for C7 were delivered by the MODIS Characterization Support Team (MCST) for science testing in March 2021 and were updated in July 2021. Overall, the reflectance differences at nadir between C6.1 and C7 are within a few percent, though the differences increase in some cases at large scan angles. The Terra visible (3, 8-12) and SWIR bands (5-7, 26) have the most significant improvements. For all other Terra bands and all Aqua bands, the C7-C6.1 differences are mostly within 1%. The C7 L1B reflectance trends will be more stable in time and have better image quality (reduced striping) compared to C6.1.

2. REVIEW OF COLLECTION 6.1 RSB CALIBRATION

The MODIS calibrated top-of-atmosphere (TOA) reflectance factor is defined as

$$\rho_{EV}\cos(\theta_{EV}) = dn^{*} d_{ES}^{2} / G(t,\theta)\ , \quad (1)$$

where $\rho_{EV}\cos(\theta_{EV})$ is the Earth view (EV) reflectance factor, dn^* is the background and temperature corrected detector signal for each pixel, d_{ES} is the Earth-Sun distance, and $G(t,\theta)$ is the instrument gain at time t and at an angle of incidence (AOI) θ of light off the scan mirror. The gain is usually written as $1/G(t,\theta) = m_1(t)/RVS(t,\theta)$, where m_1 is the calibration coefficient at the SD AOI, and RVS is the relative instrument response as a function of AOI (or scan angle) and is defined to be one at the SD. The values of m_1 and RVS combine to give the detector gains at all scans angles and these are the primary quantities related to RSB calibration that are calculated and updated frequently on-orbit through LUTs used in generating the L1B reflectance product.

The m_1 is derived using the SD calibration measurements and is computed on a band (B), detector (D), sub-frame (SF) and mirror-side (MS) basis:

$$m_1 = \frac{\rho_{SD}\cdot\cos(\theta_{SD})}{dn_{SD}^*\cdot d_{ES}^2}\cdot \varDelta_{SD}\cdot \varGamma_{SD}\ , \tag{2}$$

where ρ_{SD} is the pre-launch SD bi-directional reflectance distribution function (BRDF), θ_{SD} is the SD solar illumination angle, d_{ES} is the Earth-Sun distance during the SD calibration, dn_{SD}^* is the background and temperature corrected detector signal when viewing the SD, Δ_{SD} is the on-orbit degradation of the SD plate due to solar exposure, and Γ_{SD} is the SD screen (SDS) vignetting function.

The RVS was measured for each band during pre-launch testing. On-orbit, the time-dependent change in RVS needs to be monitored using additional calibration targets since the SD is only observed at one AOI. For most RSB, the RVS is determined from a combination of the SD measurements and regular lunar observations made through the space view (SV) port. The lunar measurements provide an accurate measure of the relative on-orbit change in the gain at the SV AOI, $G_{moon}^{oo}(t)$. Combined with the initial on-orbit SD measurements, $m_1(t_0)$, and the pre-launch RVS measurements, $RVS_{prl}(\theta_{SV})$, the absolute gain at the SV AOI is

$$\frac{1}{G(t,\theta_{SV})} = \left(\frac{m_1(t_0)}{RVS_{prl}(\theta_{SV})}\right)\frac{1}{G_{moon}^{oo}(t)}\ . \tag{3}$$

At other view angles, the gain is taken to be a linear interpolation of the values at SD and lunar AOI. Most RSB in C6.1 continue to rely on this OBC-based calibration algorithm. For a few, mostly short-wavelength bands, both the m_1 and RVS from the OBC-based calibration are inadequate due to errors in the calculation of SD degradation at short-wavelengths and the inability of the linear function to capture the full RVS effects. Supplemental data over pseudo-invariant calibration sites (PICS) in North Africa are utilized for Aqua bands 1-4, 8, and 9, and Terra bands 1-4, and 8-10. In this EV-based calibration, the at-launch SD m_1 and pre-launch RVS are still used as the absolute calibration reference at the start of mission, but the on-orbit gain trend is derived from analyzing trends of the desert data at multiple view angles to derive an on-orbit gain trend $G_{EV}^{oo}(t,\theta)$. The final EV-based calibrated gain is described by

$$\frac{1}{G(t,\theta)} = \left(\frac{m_1(t_0)}{RVS_{prl}(\theta)}\right)\frac{1}{G_{EV}^{oo}(t,\theta)}\ , \tag{4}$$

In practice, for the bands that use EV-based calibration, the OBC-based calibration using SD and moon is calculated first and then the reflectance of the desert sites is generated using the OBC-based calibration. These reflectance trends show drifts of several percent over the mission depending on band and view angle, indicating the inadequacy of the OBC-based calibration. The reflectance trends are fit over time and AOI, using the assumption of long-term reflectance stability to derive $G_{EV}^{oo}(t,\theta)$. The RVS dependence on AOI can be equivalently mapped to the view angle of the Earth scene, or the frame of the EV data sector. In this paper, we generally refer to the EV frame, which varies from 0 at beginning of scan to 1353 at end of scan, when discussing desert or other Earth view observations used for calibration.

A set of fitted m_1 and RVS forward LUTs are typically generated once a month and delivered for use in L1B production, usually timed with the collection of new lunar data. Several other LUTs are updated on a semi-regular basis for the RSBs in C6.1. These include the time-dependent uncertainty index (UI)[7] which is updated bi-annually, the SWIR out-of-band crosstalk (x_oob_1) which is time-dependent and updated bi-annually for Terra MODIS, the time-dependent quality assessment (QA) LUT, and the time-dependent pre-saturation (dn_sat) LUT.[8]

3. ALGORITHM IMPROVEMENTS

Several improvements have been discussed, tested, validated and proposed by the MCST in preparation for C7. All the major RSB algorithm improvements for C7 are described in this section.

3.1 Polarization correction for Terra bands 3, 8-10

The MODIS instrument on Terra had some modest polarization sensitivity in pre-launch testing[9] and has experienced significant on-orbit changes in the polarization sensitivity, the impact of which is mostly evident at the short wavelengths. In the C6.1 algorithm, the desert data used to derive the RVS are not corrected for polarization effects, and this has led to significant errors in the derived gain for the short wavelength bands (3, 8, 9, and 10), particularly at large scan angles. Previously, the NASA Ocean Biology Processing Group (OBPG) developed a correction to account for the polarization effects on the Terra MODIS L1B.[10,11] In C7, the OBPG coefficients are used to correct the desert data before its use in the on-orbit RVS characterization. Figure 2 shows an example of the desert data from the Libya 4 site before and after polarization correction is applied for Terra band 8 frame 1134 (near end of scan). The left panel shows the measured dn (after correction for instrument temperature and BRDF) normalized to mission start and clearly there is a large difference between the uncorrected and corrected trends, particularly for dates after 2008. For frames from the beginning of scan through nadir, the polarization correction has little impact. The right panel shows the normalized reflectance trends, where the reflectance is calculated with the OBC-based algorithm. Since these data trends are fit as part of the process of generating the m_1 and RVS LUTs, the use of polarization-corrected data results in changes of several percent in the L1B gains.[12] In comparison, the short wavelength bands of Aqua MODIS have not shown any changes in the polarization sensitivity on-orbit. Therefore, no correction for polarization effect has been applied to the desert data before its use in the on-orbit RVS characterization.

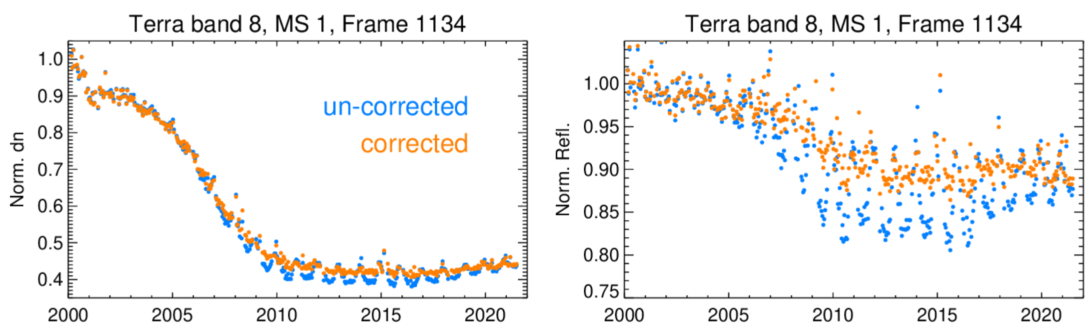

Figure 2. Trends of normalized dn (left) and normalized reflectance (right) from the Libya 4 desert site for Terra band 8 mirror side 1 frame 1134 (near end of scan) with and without polarization correction. The reflectance is calculated using the OBC-based calibration.

3.2 Fitting improvements to desert-based calibration

Within the current C6.1 algorithm, desert PICS in North Africa are used for certain RSBs to compensate for drifts seen in reflectance at AOIs far from the SD and SV AOIs.[3] These bands include Aqua bands 1-4, 8, and 9 and Terra bands 1-4, and 8-10. While this desert-based calibration has shown significant improvement over utilizing the OBCs alone, several tests have been performed within MCST to continue to enhance this approach and are incorporated within C7. We already described in Section 3.1 the addition of polarization correction to the desert observations for Terra bands 3, 8-10 prior to using the observations in the calibration algorithm. In this subsection, we describe how the desert trends are processed and fit within the calibration algorithm, after the initial BRDF correction and polarization correction. The changes include the use of more frames of data from each desert site in the analysis, fitting over frame first, and using a sliding window average to improve the time fitting. These fitting changes apply to all bands that use the desert data for both Terra and Aqua.

The first improvement being made for the C7 desert-based RVS approach is the use of extra frames from the PICS. Currently in C6/C6.1, data from the Libya 1, Libya 2, and Libya 4 sites are used in the calibration, but only a handful of the available frames from each site are used,[8] which were carefully selected during the initial C6 tests. Over time, the use of more frames has been found to improve the quality of fitting over frame. In C7, all cloud-free desert observations from these same three sites are used, covering 14-15 consistent view angles from each site.

The desert-based technique[3] that is implemented in C6/C6.1 first fits the desert data (the EV dn after correcting for instrument background, temperature, Earth-Sun distance, and site BRDF using an empirical model) over time at each of the selected frames. These fitted curves at each frame are then combined and a fit over frame is performed at a series of times, giving the on-orbit gain change as a smooth function of frame and time over the mission. This method relies upon the 16-day repeatability of the data at each of the desert PICS at the specified frames used in the current collection. However, at some point in both missions, the satellites will be taken out of their current orbit and allowed to drift. This 16-day repeatability will no longer be reliable as both MODIS instruments will view these desert PICS at other frames during this period. To prepare for this, C7 will begin implementing a technique in which the PICS data are binned each month, fitted with respect to frame first, and then fitted with respect to time (normalized to mission start).[13] Figure 3 shows an example of the initial, monthly-binned fit over frame for the Libya 1, 2, and 4 PICS separately. After each site is treated independently, the fitted EV dn data are then combined and fit with respect to time. Then, the results of the time fitting from all three sites are combined and fit together over frame one last time in order to get the coefficients of the m_1 and RVS LUT. While this simple fitting change was made in preparation for the constellation exit, more work is still required to improve the BRDF correction and/or atmospheric corrections used for these desert PICS in order to continue using this calibration algorithm during orbit drifting. For Terra band 10, in the first 3000 days of the mission (through 2008), only the Algeria 3 site is used to derive the desert-based calibration in C7, due to saturation of this high gain band over the Libya sites in early mission. For this initial time period, the data is processed using the previous approach: fitting first over time and then over frame. After day 3000, Terra band 10 uses the data from the three Libya sites and the same algorithm as all of the other bands.

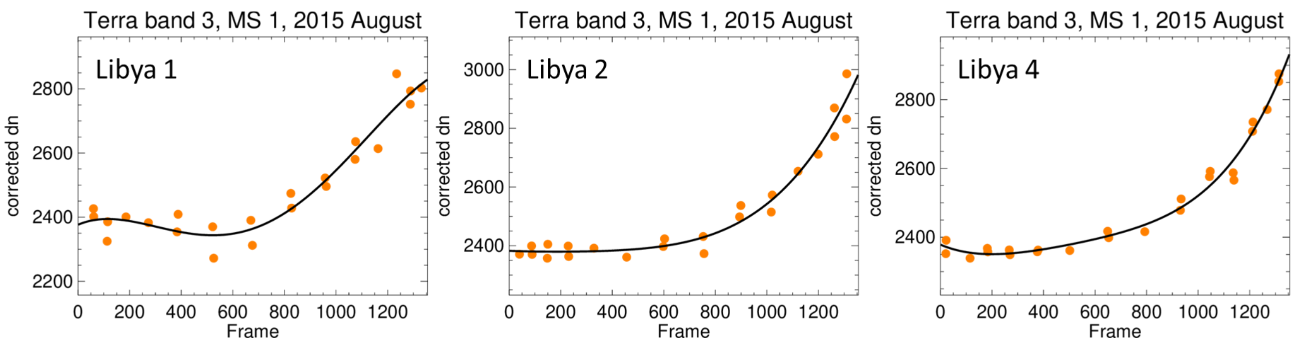

Figure 3. Examples of monthly-binned frame fit for Terra band 3, MS 1, August 2015, for (left) Libya 1, (middle) Libya 2, and (right) Libya 4. Each orange point is a single observation of the site and the black lines are quartic fits.

The last algorithm change to the desert-based calibration within C7 is the use of a sliding-window average (SWA) for the time fitting. Currently in C6/C6.1, the time-fitting method utilizes piecewise fitting segments to fit the desert reflectance over time. However, due to some inadequacies in the previous fits and to simplify the fitting procedure, a SWA method is used and results in some improvement in the quality of the fits.[14] After the initial fitting over frame, the fitted values of adjusted dn are multiplied by the m_1/RVS values derived using the OBC-based calibration to get reflectance trends. Figure 4 shows examples of these reflectance trends for Terra band 3, normalized to mission start, with the SWA fitting curve on top of the data. In the plots, the orange points are the result of the initial fitting over frame (one point per monthly bin).

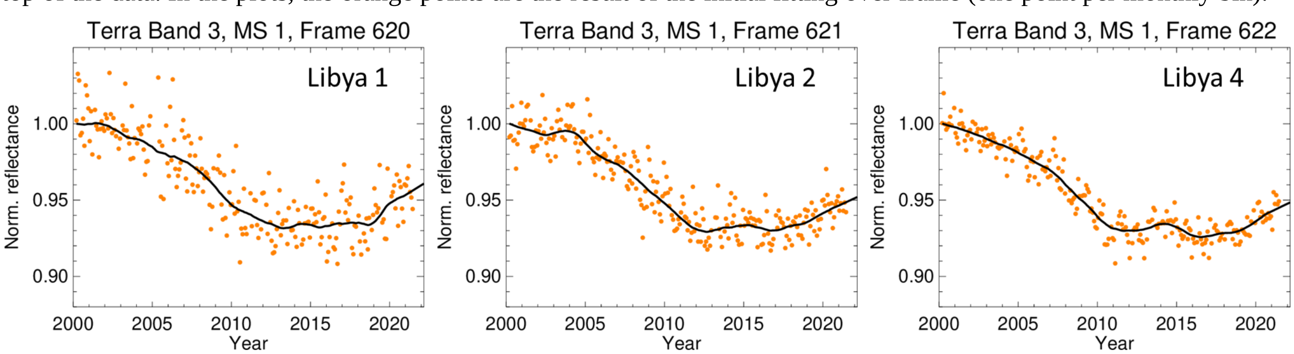

Figure 4. Desert site reflectance normalized to mission start for Terra band 3 mirror side 1 at frames near nadir for (left) Libya 1, (middle) Libya 2, and (right) Libya 4. The reflectance is calculated using the OBC-based calibration. Orange symbols are the result of the monthly-binned fit over frame and black lines are the final time fits from combining the linear fits and the SWA.

For the fitting strategy, the SWA fitting is calculated over the mission using a 2-year averaging window for most bands and a 3-year or 4-year averaging window for the Terra SWIR bands that use DCC data (see Section 3.4). The SWA at any point in time is only calculated when a full window of data is available. For example, near the beginning of the mission, for a 2-year SWA, the SWA results begin to be calculated one year after mission start since prior to that time there are not enough data to do a centered 2-year SWA (one-year before to one-year after). For this beginning time period, and also the time period at the end of the data set, a linear fit is performed using a few years of data to determine the fitted curve in the missing region of time. The number of years of data used to calculate this linear fit is in the range of 3 years to 7 years, varying by band. The linear fits at the ends are smoothly connected to the SWA result. In Fig. 4, the black curves are the combined result of the linear fits and the SWA. Three examples of the fitting are shown in Fig. 4, one for each of the three sites and all for Terra band 3 mirror side 1 at a frame near nadir. The variance in the data is largest for the Libya 1 site and smallest for the Libya 4 site, but in all three cases the black fitted curves are very similar and pass smoothly through the center of the data points.

As already stated, the results of the time fitting from the three sites are combined and fit over frame together to derive the m_1 adjustment and the coefficients of the RVS LUT. Examples of the final, combined fit are shown in Fig. 5, again for Terra band 3, showing generally good agreement between the three sites. As in C6/C6.1, the final fit over frame is constrained to match the lunar calibration results at the AOI of the SV (frame 17) for all desert-based bands except bands 1 and 2.

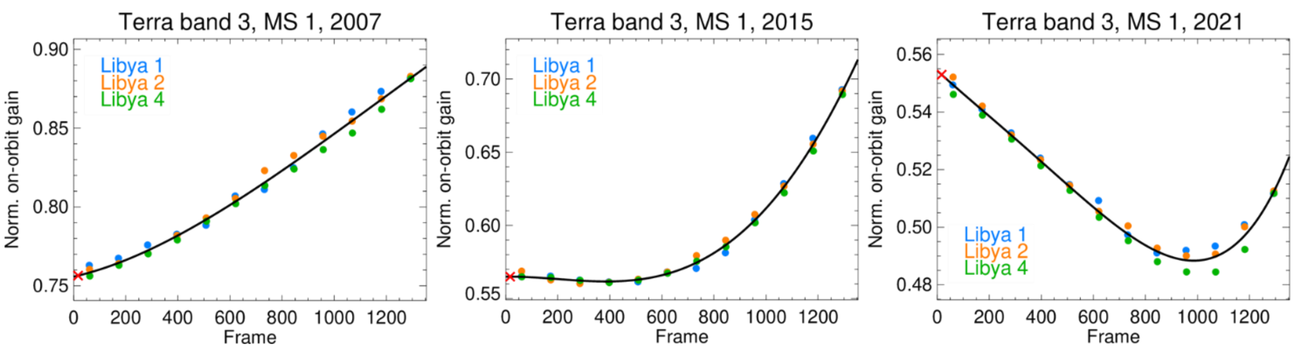

Figure 5. Final, combined fit over frame to determine the on-orbit gain for Terra band 3 mirror side 1 in years 2007 (left), 2015 (middle), and 2021 (right). The red "x" near the beginning of scan is the result of lunar calibrations and the fit is constrained to go through this point.

3.3 Terra SWIR out-of-band response and crosstalk

The Terra MODIS SWIR bands have a known issue related to a 5.3 μm out-of-band (OOB) thermal leak, along with an electronic crosstalk, that was identified prelaunch. The crosstalk correction algorithm implemented in the MODIS L1B calibration process since launch utilizes the regularly scheduled nighttime-day-mode observations to derive the crosstalk coefficients that are used to correct the gains (from SD) as well as the uncalibrated EV response.[15] Based on early observations from the MODIS Airborne Simulator field campaigns,[16] band 28 (7.325 μm) was chosen as a surrogate sending band for Terra MODIS to simulate the OOB radiances as MODIS does not have a spectral band centered at 5.3 μm.

In recent years, the Terra MODIS photovoltaic (PV) long-wave infrared (LWIR) bands' (27 to 30) electronic crosstalk increased considerably, especially following the spacecraft safe mode event in February 2016.[17] This accentuated degradation in the PV LWIR performance also degraded the performance of the SWIR crosstalk correction and the SWIR band calibration and data quality. The use of band 25 (4.52 μm) as a sending band, also employed in Aqua MODIS, largely mitigates these artifacts and improves the on-orbit gain stability for the SWIR calibration, along with reducing detector-to-detector and subframe-to-subframe striping in the calibrated imagery.[18] The switch of Terra SWIR sending band from band 28 to band 25 was made in C6/C6.1 forward production starting in mid-2019. In C7, band 25 is used as the sending band for the entire Terra mission. In the case of Aqua MODIS, where the artifacts due to crosstalk are significantly smaller, band 25 is currently used as a sending band and, based on the excellent on-orbit performance, no change is proposed for C7.

3.4 Time-dependent RVS for Terra SWIR bands

As stated above, band 25 will be used as the reference band for the Terra MODIS SWIR crosstalk correction for the entire mission in the C7 LUTs. After making this change, the SD calibration is evaluated in the same manner as before, and the measured SD-derived m_1 values are fitted to piecewise polynomial functions of time to get the initial m_1 LUTs. For the SWIR bands in all previous MODIS Collections, the pre-launch RVS LUTs have been used for the entire mission, with no on-orbit correction to the RVS. For C7, we use the Earth-based calibration algorithm for the SWIR bands to derive a time-dependent RVS and a time-dependent correction to the SD m_1 values. This is the same general strategy currently used in C6.1 for the short-wavelength bands, except that the SWIR bands in C7 use DCC as the data source rather than the desert PICS used for the short-wavelength bands. A time-dependent RVS is applied for bands 5 and 26, which show up to 2% and 0.5% change in RVS on-orbit, respectively. Bands 6 and 7 continue to show stable RVS and will continue to use pre-launch RVS in C7. The time-dependent gain correction is applied to m_1 for all four SWIR bands.

We primarily use DCC as a stable reference for evaluating the reflectance product performance for all SWIR bands: 5, 6, 7, and 26.[19,20] We also use the PICS from the Libyan desert to evaluate the performance of bands 5, 6, and 7 (the desert observations do not provide useful data for band 26). Both targets show consistent trends that agree well with each other for bands 5, 6, and 7. For C7 calibration, we follow our previously developed methods for identifying DCC pixels and generating trends of the corrected signal level from DCC for each band and mirror side (averaged over all detectors and sub-frames) using mission-long x_oob_1 tables from reference band 25 to perform the crosstalk correction. The DCC pixels are binned into 13 frame zones across the MODIS scan range to track the signal changes across frame and derive the RVS. No BRDF correction is currently applied for the SWIR bands.

Before using the DCC trends to derive gain corrections, the corrected signal is converted to reflectance using the fitted SD m_1 and the pre-launch RVS. Note that lunar observations are not used to derive on-orbit RVS for the SWIR bands due to complications with the crosstalk correction.[21] This contrasts with the EV-based calibration procedure for the shorter-wavelength bands, which use the SD m_1 and the OBC-based RVS (from combining SD and lunar data) as the baseline for calculating the desert reflectance drift prior to doing the time fitting and deriving the corrections (Section 3.2).

The resulting reflectance trends are fit first over time and then over frame to derive the on-orbit gain change. An example of the time fitting is shown in Fig. 6 for three different frame zones of band 5 mirror side 1. A start time of day 820 (epoch 2000) is used as the normalization point for the on-orbit time fitting for all SWIR bands and frames. This means that the gain is assumed to follow the SD m_1 exactly through day 820 with no on-orbit RVS change. This is expected to be a good assumption and avoids processing challenges caused by the large gain changes seen in the Terra SWIR bands in early mission due to multiple electronics configuration changes. The trends are fit over time using a SWA algorithm that is the same as what we use for the desert data and is described in Section 3.2. After fitting the trends from 13 frame zones over time, the fitted values are fit over frame using a quadratic function for band 5, a linear function for band 26 and a simple mean for bands 6 and 7. In other words, no time-dependent RVS is applied to bands 6 and 7. Examples of the frame fitting in year 2016 are shown in Fig. 7 for each band. When the RVS and m_1 corrections are derived from these fits, the results of the two mirror sides are averaged together, so that the RVS has no mirror side dependence and the final m_1 mirror side differences are equivalent to the SD m_1 mirror side differences. The new algorithm effectively forces the C7 calibration to produce flat reflectance trends when evaluated with the same DCC targets. Bands 5 and 26 show a gradually increasing RVS on-orbit, with the end-to-end on-orbit RVS changing up to 2% for band 5 and 0.5% for band 26. Bands 6 and 7 do not show any significant change in RVS and thus continue to use the pre-launch RVS. The EV-based correction to m_1 LUTs is applied to all four SWIR bands.

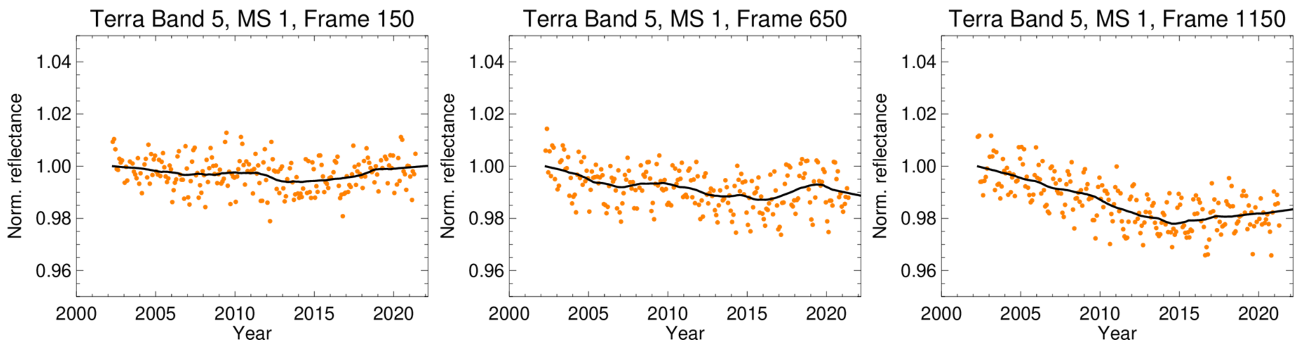

Figure 6. Normalized reflectance trends from DCC using SD m_1 and pre-launch RVS for Terra band 5 mirror side 1 (a) frame 150 (near beginning of scan), (b) frame 650 (near nadir), and (c) frame 1150 (near end of scan). Orange points are monthly measured values and black lines are the fits.

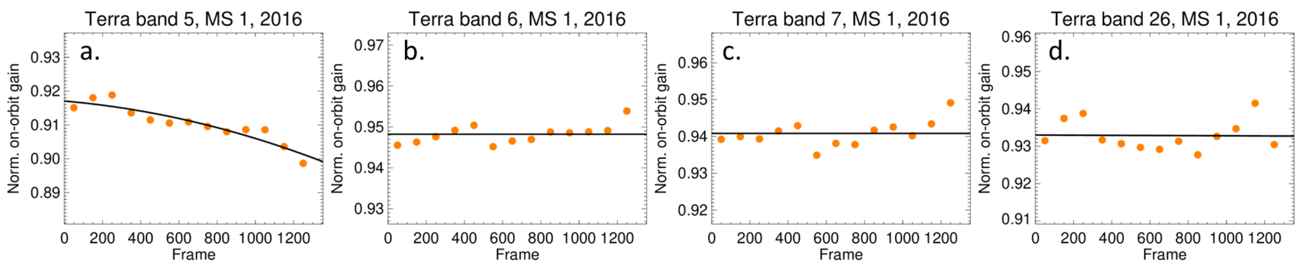

Figure 7. Examples of final fitting of DCC data vs frame in year 2016 for mirror side 1 for (a) Terra band 5, (b) band 6, (c) band 7, and (d) band 26. Orange points are the values from time-fitting in 2016 and black lines are polynomial fits: quadratic for band 5, linear for band 26, and mean for bands 6 and 7.

For Aqua MODIS, SWIR bands in C7 will continue to use band 25 as the reference band for crosstalk correction, SD-based m_1, and pre-launch RVS, as was done in Collection 6 and C6.1. DCC and desert reflectance trends have been studied and they continue to show stable performance of this calibration with no on-orbit change in RVS. Therefore, no EV-based calibration corrections will be used for Aqua SWIR bands.

3.5 Interband calibration for Terra bands 11 and 12

The degradation of the solar diffuser, together with the lack of OBCs to cover additional scan angles other than the one for the lunar observations, has resulted in the use of Earth view responses from the PICS to track the on-orbit RVS changes.[3] This approach has been implemented in C6 and C6.1 for bands 1-4, 8 and 9 of both instruments and additionally for band 10 of Terra MODIS. As the missions continue to operate over a decade beyond their designed lifetimes, and the SD continues to degrade, it is expected that the OBC-based calibration currently applied to other bands, specifically the high-gain ocean bands, will be inadequate to maintain the long-term calibration stability. An interband calibration approach has been formulated and will be implemented in C7. The proposed approach relies on the use of a spectrally-matching stable reference band to evaluate the long-term calibration stability of the high-gain ocean bands that typically saturate while viewing the desert PICS. Ocean reflectance trends are constructed using a ratio of the target ocean band (e.g. band 12) with a reference band (e.g. band 4), and the assumption that the calibration of the reference band is accurate. Results from this approach indicate a noticeable reflectance drift for Terra MODIS bands 11 and 12 using the C6/C6.1 calibration (OBC-based calibration), whereas the Aqua bands continue to show excellent temporal stability.[22] In C7, the ocean reflectance trends from the interband calibration approach are first fit in time using the SWA approach described in Section 3.2 and then fit over frame to derive a correction to both the m_1 and RVS LUTs. Examples of the time fitting are shown in Fig. 8 for Terra band 12. Similar to the calibration algorithm for most bands that use the desert data, the fit over frame is constrained to go through the lunar data at the lunar frame. This correction will be applied only to Terra bands 11 and 12, with an impact of up to about 3% (see Section 4).

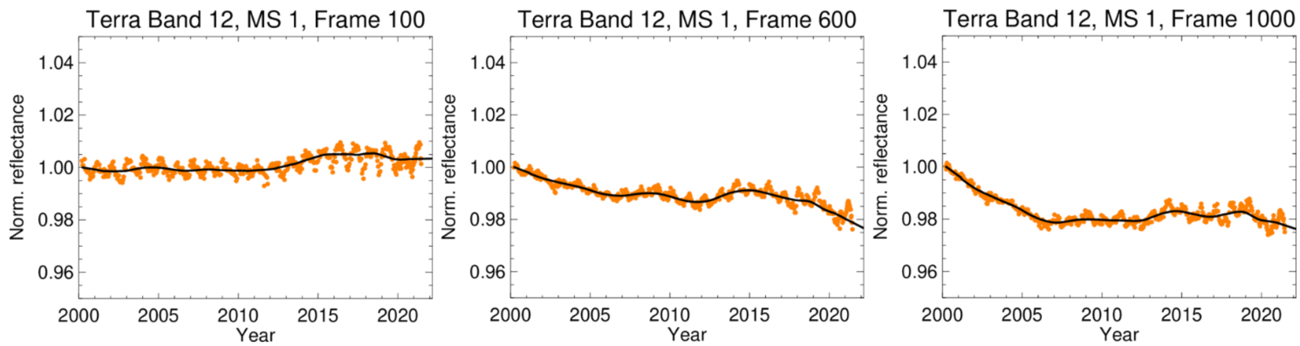

Figure 8. Normalized reflectance over ocean scenes of Terra MODIS band 12 mirror side 1 for frames near beginning of scan (left), near nadir (middle) and near SD AOI (right). Orange points are reflectance calculated using an interband calibration approach with band 4 as a reference band and using the OBC-based calibration for bands 11 and 12. Black lines are the result of the SWA fitting algorithm.

3.6 Aqua VF improvements

The MODIS high-gain ocean color bands (8-16) are calibrated with the SDS closed to avoid saturation. Therefore, the characterization of the vignetting function (VF) of the SDS is necessary for calibrating the detector gain coefficients of these bands. Due to the lack of pre-launch characterization, a series of yaw maneuvers were carried out on-orbit for both Terra and Aqua to enable its characterization early in their missions. The VF currently used in C6 and C6.1 was derived from the yaw data of low-gain bands 3, 4, 18, and 19, and is applied to the high-gain ocean color bands with the assumption that all spectral bands should have the same VF. Any VF error introduced by this method has been carried over into the gain coefficients calibrated with the SDS closed for these high-gain bands. More recently, a different approach was used to derive the VF from the yaw maneuver data that takes into account the frame-level mismatch between different detectors' footprints on the SD. A set of band- and detector-dependent VFs of all bands are derived from the VF of any reference low-gain band by applying proper SD image frame adjustments.[23] The implementation of this improved VF into the C7 calibration of the ocean color bands effectively reduces the undesired detector-dependent seasonal oscillation observed in the long-term trending of their gain coefficients. Figure 9 shows the trends of measured SD m_1 values over the mission for detector 6 (product order) of Aqua bands 14 and 16 before (C6.1) and after (C7) the implementation of the new, detector-dependent VF. The reduction in the seasonal oscillations of the gain trends allows for more accurate short-term tracking of gain changes and more accurate forward prediction but does not significantly change the long-term (multi-year) gain trends. Though there is a clear offset between the two versions in the plot for this detector, the band-average m_1 values at the start of mission are identical for C6.1 and C7.

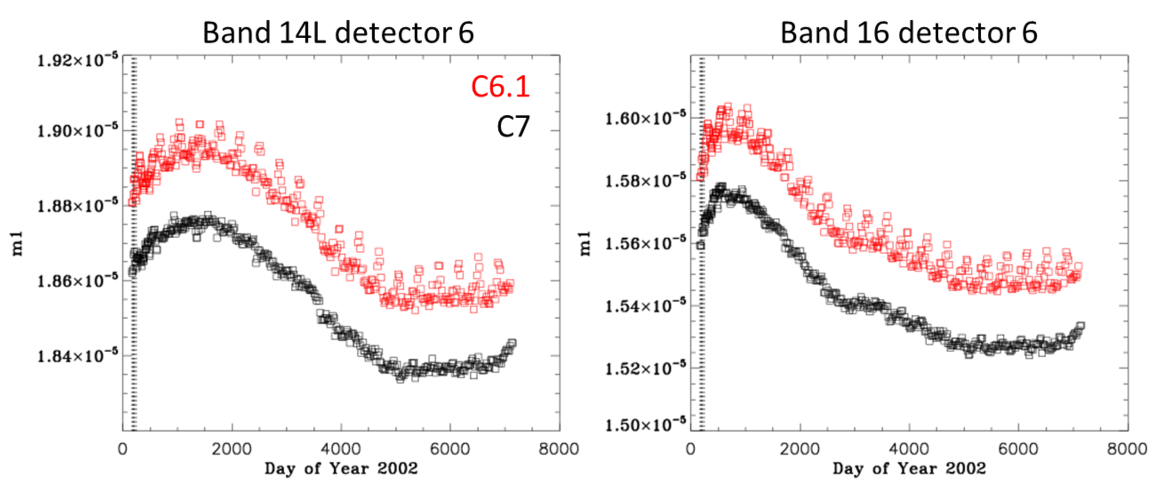

Figure 9. Entire-mission reprocessed SD m_1 for C6.1 compared to C7 for band 14 low gain (left) and band 16 (right) mirror side 1 center detector.

3.7 Extend detector-dependent RVS to Terra band 4

The on-orbit change in RVS for most bands is defined separately for each band and mirror side, but all detectors within a band have the same RVS values. In C6/C6.1, a handful of bands are an exception to this, and use a detector-dependent RVS function: Terra bands 3, 8-12 and Aqua bands 8-12.[3] In addition to these bands, Terra band 4 will also use detector-dependent RVS in C7. The same algorithm for detector-dependent RVS will be used in C7 as is currently used in C6/C6.1. This algorithm involves first applying a correction to the detector differences of the measured SD m_1 values and then calculating a two-point detector dependent RVS from the SD and lunar data. For the SD m_1 correction, the reflectance of ocean scenes is calculated at the SD AOI using the SD m_1 data. A correction is derived that removes any detector differences in this ocean reflectance and that correction is applied back to the SD m_1 data before it is used in the RVS and m_1 LUT derivations. For the RVS, the detector differences from the lunar observations and the adjusted SD observations are combined to derive a two-point linear RVS function at the detector level. We recently used detector differences observed in DCC reflectance to evaluate the calibration performance for Terra and Aqua bands 1, 3, and 4.[24] Terra band 4 was found to show improved stability and reduced striping in the DCC reflectance product when the detector-dependent RVS algorithm is applied. For Aqua bands 3 and 4, the current band-average RVS algorithm continues to give excellent performance in the DCC trends, so there is no need for a detector-dependent RVS correction.

3.8 Re-processed LUTs generated using consistent algorithms

The C6 L1B product, which began production in 2012, included several improvements to the RSB LUTs.[3] One such improvement was the use of desert PICS for the RSB characterization of the shorter wavelength bands (1-4, 8, 9). Over the course of C6 however, band 10, calibrated using the OBC-based RVS alone, began showing drifts in its reflectance. Therefore, starting in May 2014, the MCST initiated the use of desert PICS for this band as well within C6 forward production. While Terra bands 1-4, 8 and 9 utilize the Libya 1, 2, and 4 PICS for their desert-based RVS characterization, Terra band 10 exhibits saturation at these PICS before March 2008. Therefore, Terra band 10 utilizes the Algeria 3 PICS within the desert-based RVS before this time, with the Libya PICS used after this time. For the C7 product, Terra band 10, along with the other short wavelength bands, will be reprocessed from the start of the mission utilizing the EV-based RVS approach. Also note that the desert data used for Terra band 10 in C7 will be corrected for polarization (see Section 3.1). Similar updates include the desert-based calibration for Aqua bands 1-4 that was implemented for the entire data record in C6.1 but not in C6, and a partial reprocessing of Terra bands 1 and 2 in C6.1.

More generally, all calibration LUTs are regenerated for C7 using consistent algorithms and fitting strategies over the entire MODIS missions. This will improve the quality of the LUTs and reduce noise and errors associated with the inaccuracies of forward prediction which exist in the C6/C6.1 LUTs from the start of production in 2012 through the current date. We also note that a slightly different lunar calibration method is used to derive the C7 RVS LUTs. The C7 lunar calibration will use only scans which view the full disk of the Moon, as opposed to the current approach in C6.1 that generates images of the Moon for each detector by combining the results of all scans with a partial view of the Moon.[25] The change results in a slightly smoother long-term trend of the lunar results, particularly for the mirror-side ratio, but does not have a significant impact on the long-term RVS calibration.

In addition to the already-discussed changes to the m_1, RVS and x_oob_1 LUTs, minor changes were also made to the LUTs for the detector QA, E_{sun}, and DN_{sat}. The QA LUTs for C7 RSB are identical to the C6.1 RSB, except for two detectors in Terra band 5. In C6/C6.1, detectors 3 and 5 (product order) of Terra band 5 were flagged as out-of-family gain starting in March 2019 (with a LUT timestamp of 2017/296). After continued evaluation of their performance, it was determined that a flag of noisy was more appropriate and the QA flag was changed to noisy starting 2021/035. In C7, Terra band 5 detectors 3 and 5 are flagged as noisy starting from the 2017/296 timestamp. The E_{sun} LUT provides the values of solar spectral radiance integrated over the RSR of each individual detector for use in converting the reflectance product to radiance and are included in each L1B granule. The E_{sun} values have been re-calculated for C7. Though the solar spectral radiance LUTs and RSR LUTs have not changed, a slight discrepancy was found between the recalculated values the values currently in the C6/C6.1 LUTs. The reason for the discrepancy is not known. The re-calculated E_{sun} values are used in the C7 LUTs and L1B. The only impact is a shift in the band 1 radiance product of about 0.5% for both Terra and Aqua MODIS, but the reflectance product is not affected. No other bands see any impact from the E_{sun} LUT change. The time-dependent DN_{sat} LUTs give the DN values at which saturation begins to occur, which for a few bands can be less than the nominal value of 4095. We use histograms from one orbit of Level 1A data to assess the saturation threshold and derive values of DN_{sat}. The LUTs have been updated periodically throughout C6/C6.1 production. For C7, the same basic algorithm is used to determine the DN_{sat}values, but with some improvements to provide smoother trends and more consistent LUT updates throughout the missions. The impact on L1B products should be very minimal and only at the extreme high end of the radiance range where the number of valid pixels might change.

4. IMPACT ASSESSMENTS AND COMPARISON WITH C6.1

In this section, we review the cumulative impact on the L1B reflectance products of the RSB algorithm changes discussed in Section 3. For bands that have multiple algorithm changes applied, the impacts of these changes are of course coupled together, e.g. the polarization correction and the fitting changes to desert data used for short-wavelength Terra bands. In general, the overall, combined impacts of the changes are most significant for the Terra MODIS short-wavelength bands 3, 8-12, and SWIR bands. For other Terra MODIS RSB and for all Aqua MODIS RSB, the overall differences in gain and reflectance between C6.1 and C7 are generally within 1% and there are no major impacts expected on the downstream products.

4.1 Changes in long-term trends

As part of the evaluation of the cumulative gain changes, we show the ratio of the calibrated m_1/RVS (inverse gain) between the C7 LUTs and the delivered C6.1 LUTs as of July 2021. Figure 10 shows the entire mission m_1/RVS ratios (C7 divided by C6.1) for all Terra RSB for mirror side 1, averaged over all detectors and subframes within a band. The values are shown at a few select years over the mission and at three different scan angles to demonstrate the combined changes to both m_1 and RVS: -45° (equivalent to frame 123), nadir (frame 677) and +45° (frame 1230). The m_1/RVS differences are equivalent to the differences that will exist in the L1B reflectance products between C7 and C6.1. A similar chart for Aqua MODIS at nadir is shown in Fig. 11.

By far the most significant impact on the calibrated gains and thus the L1B reflectance comes from the use of polarization-corrected desert data in deriving the RVS for Terra bands 3, 8, 9, and 10, so these bands show the largest deviations from one in Fig. 10. For frames near the beginning of scan through nadir, the differences between C7 and C6.1 are relatively minor for bands 3, 8, 9, and band 10 after 2014. However, near the end of scan, the impact can be much larger – more than 10% at certain times for band 8. For band 10 before 2014, the C6.1 calibration used only the OBC-based algorithm and the desert data was only included in forward production after 2014, which is the reason for the large differences at nadir and at +45° scan angle in that time period. In C7, the desert-based calibration with polarization correction and the new fitting approach is applied from mission beginning. The gain differences shown in Fig. 10 are the impact of using polarization-corrected desert data on the calibrated gains, and by extension the L1B reflectance. It is important to note, though, that there is no polarization correction applied to the L1B data itself, since this would be a scene-dependent correction. Also, the impact on downstream science products will not be this significant since there are already polarization mitigation strategies in place in C6.1. The primary goal and impact of this change is to improve the accuracy of the L1B reflectance and reduce the magnitude of the downstream corrections that need to be applied on top of the L1B reflectance. Figure 12 shows the normalized reflectance at the Libya 4 site for Terra band 8 using C6.1 compared to C7 LUTs for a near-nadir frame and a frame near end of scan. Near nadir, there is little difference in the long-term trends between the two Collections, but near of scan there are large errors in the C6.1 LUTs since the desert data was not polarization-corrected when deriving the LUTs (see Fig. 2). Similar improvements are seen in the C7 desert reflectance trends for bands 3, 9, and 10.

The changes made to the Terra SWIR bands, to improve the crosstalk correction (using band 25 as the reference band) and to introduce an on-orbit RVS for bands 5 and 26, also result in a relatively significant change in the reflectance in C7 relative to C6.1, and this can also be seen in Fig. 10. The C7 Terra SWIR band-averaged gain near nadir is not significantly different from C6.1, with differences within 1% for dates through 2015. For dates after the February 2016 safe mode event, the previous C6.1 calibration using band 28 had significant errors, so a larger difference up to a few percent is seen between C6.1 and C7 in this time period. Also, for bands 5 and 26, the inclusion of on-orbit RVS results in gain differences at other frames of up to 2% for band 5 between C6.1 and C7, with the difference growing gradually over the mission. Figure 13 shows the normalized reflectance over DCC for Terra band 5 at three different frames and for Terra band 26 near nadir. In all four cases presented, the C6.1 reflectance trends have significant upward drift that is corrected in C7. We also evaluate the reflectance trends over desert sites for SWIR bands 5, 6, and 7. Overall, the C7 reflectance trends will be more stable across all frames compared to C6.1.

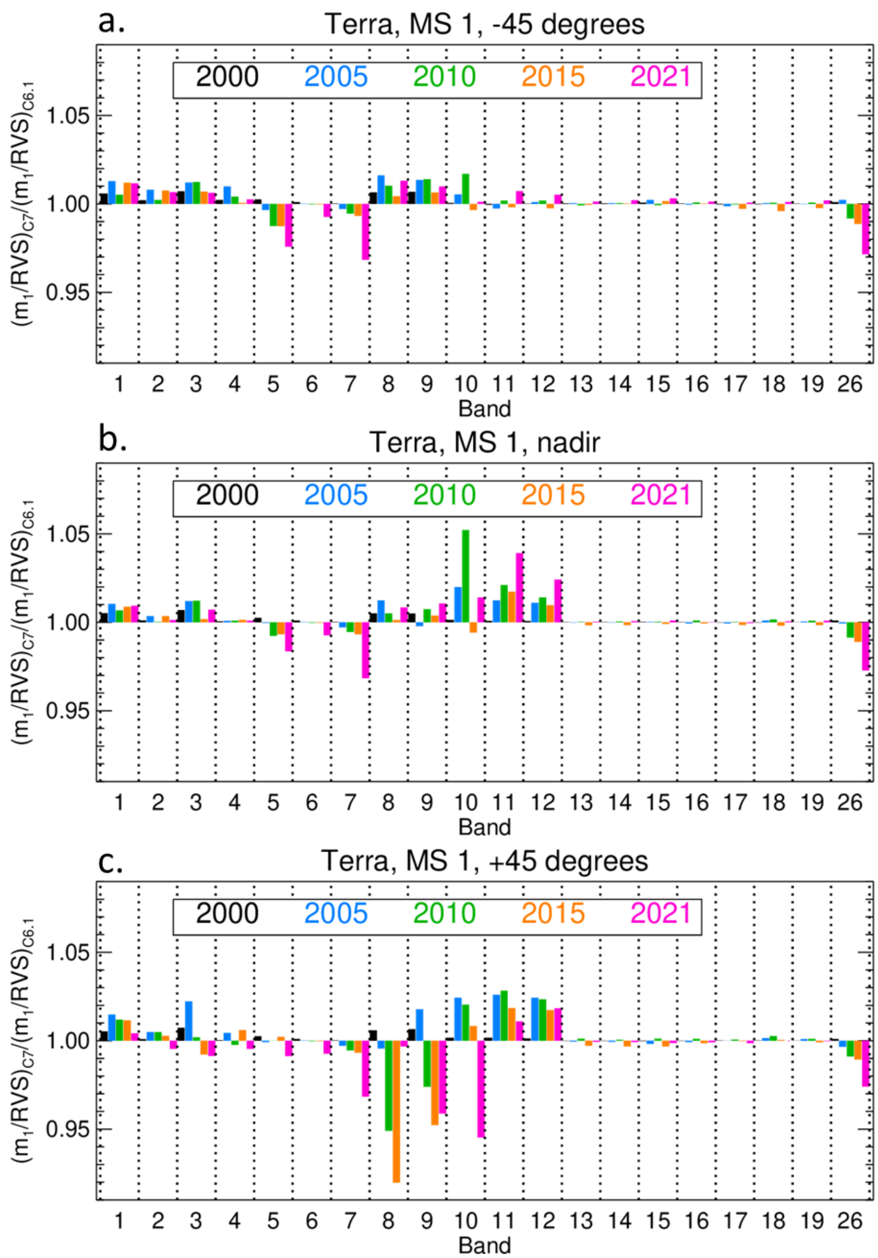

Figure 10. Ratio of calibration factor m_1/RVS from C7 to C6.1 for all Terra RSB mirror side 1 at a few select years over the mission for (a) -45° scan angle, (b) nadir, and (c) +45° scan angle.

Terra bands 11 and 12 use the OBC-based calibration in C6.1 and the ocean interband calibration in C7. The m_1/RVS C7/C6.1 ratio in Fig. 10 shows relatively little difference near beginning of scan (-45°) since the Moon is used as the calibration reference near this frame in both versions, but a deviation of up to about 3% is seen for both bands at nadir and larger frames. For the remaining bands that use desert-based calibration – Terra bands 1, 2, and 4 and Aqua bands 1-4, 8, and 9 – the changes in the algorithm used to fit the desert data (Section 3.2) have minimal impact on the long-term gain trends. The m_1/RVS differences are within 2% at any point in time across all frames, and any changes in long-term reflectance trends between the two versions are within 1%.

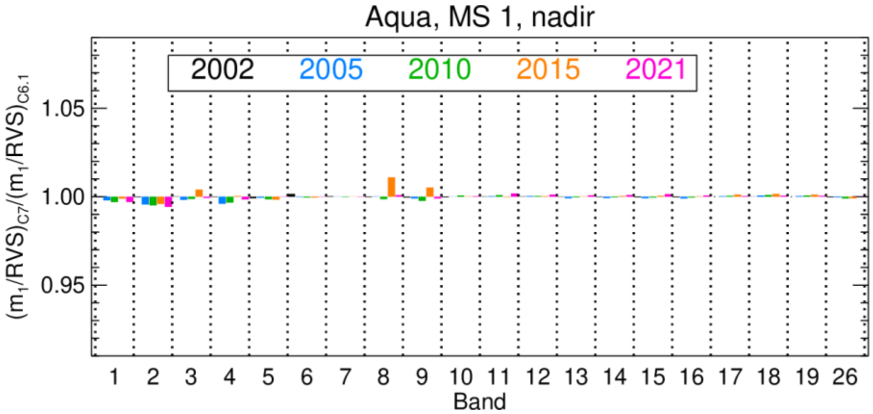

Figure 11. Ratio of calibration factor m_1/RVS from C7 to C6.1 for all Aqua RSB mirror side 1 at a few select years over the mission at nadir. Note that the plot scale is the same as in the Terra charts in Fig. 10.

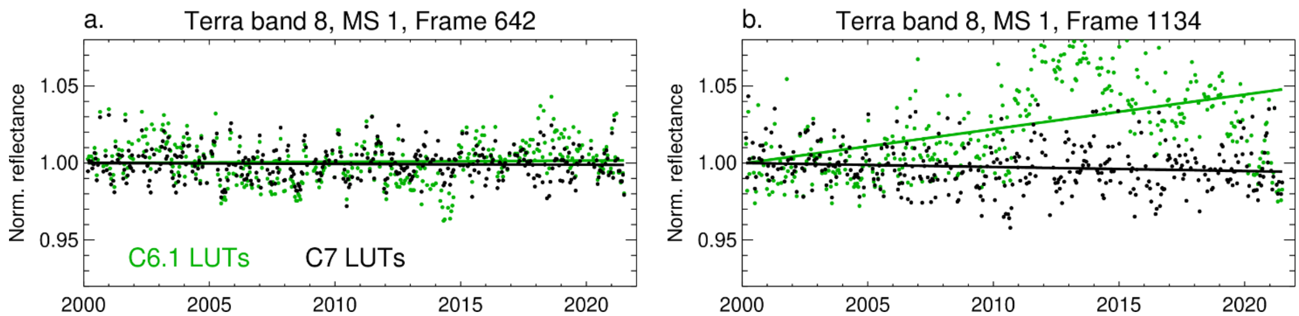

Figure 12. Terra reflectance trends from Libya 4 for C6.1 LUTs compared to C7 LUTs: (a) band 8 near nadir; (b) band 8 near end of scan. Data points are individual observations and lines are a linear fit over the mission, with both data and fit normalized to the fitted value at mission start.

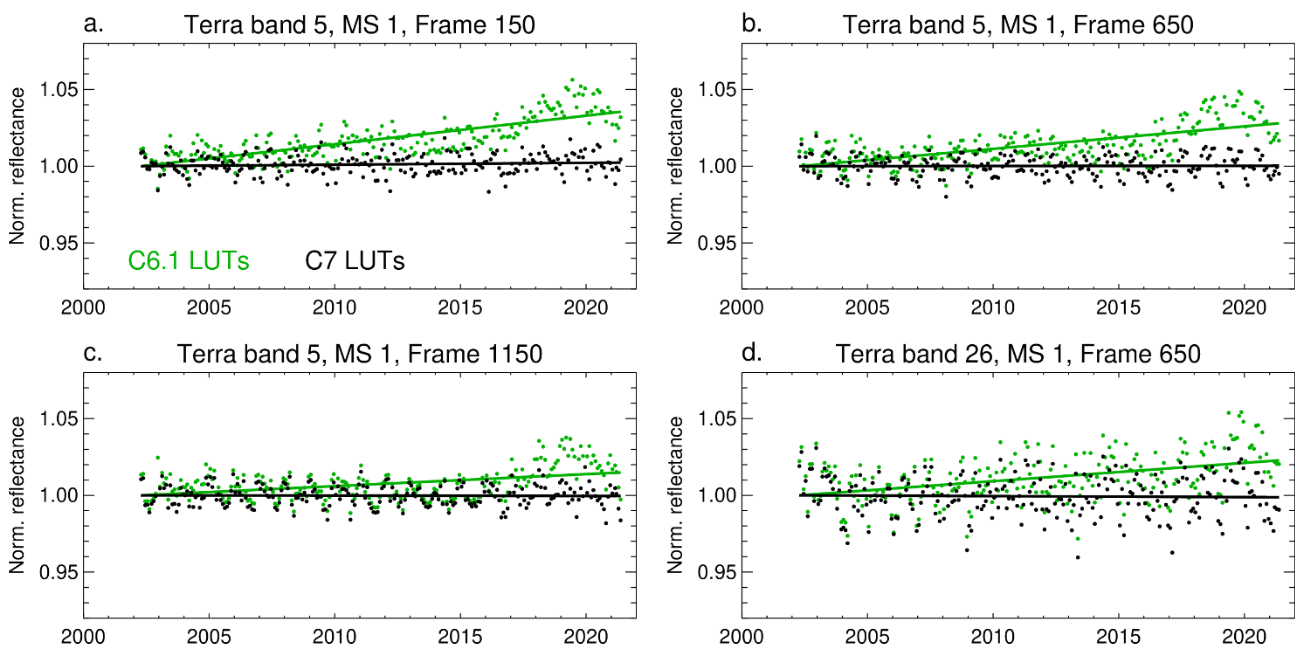

Figure 13. Terra reflectance trends from DCC for C6.1 LUTs compared to C7 LUTs: (a) band 5 near beginning of scan; (b) band 5 near nadir; (c) band 5 near end of scan; (d) band 26 near nadir. All panels show mirror side 1 trends. The trends for mirror side 2 are similar. Data points are monthly DCC measurements and lines are a linear fit over the mission, with both data and fit normalized to the fitted value in 2002 (data before 2002 is ignored for this plot).

For the rest of the RSB, there are no major algorithm changes between C6.1 and C7 and the m_1/RVS ratio plots in Figs. 10 and 11 show little difference, within 1%. In many cases, there are short time periods after the start of C6 (2012) where the C7/C6.1 differences are up to 2% or so even for bands with no major algorithm changes. This is due to short-term errors in the forward predicted LUTs used in C6.1. The C7 LUTs are reprocessed over the entire mission with consistent algorithms, which will correct these slight deviations. Some of the C7 algorithm changes, such as the VF improvements for Aqua and the fitting enhancements applied to the desert data for both instruments, reduce the noise in the calibration time series trends and allow for more accurate tracking of the gain over short time periods within the mission. This will also lead to more accurate gain prediction once C7 LUTs are being generated in forward production.

4.2 Image quality improvements

In addition to more accurate long-term gain and reflectance trends, another significant impact of the crosstalk sending band switch for Terra SWIR bands is a dramatic improvement in the sub-frame (along-scan) and detector (along-track) striping throughout the mission and especially for dates after the February 2016 safe mode event. Figure 14 shows an example image of the 500 m resolution L1B radiance from April 7, 2016 for band 6 using C6.1 compared to C7 LUTs. The C7 case has a clear improvement in image quality, especially noticeable toward the right edge of the image. Horizontal and vertical line scans show the significant reduction in along-scan and along-track striping. The sending band switch and resulting improvements in image striping have also been included in the C6.1 forward product since August 2019.

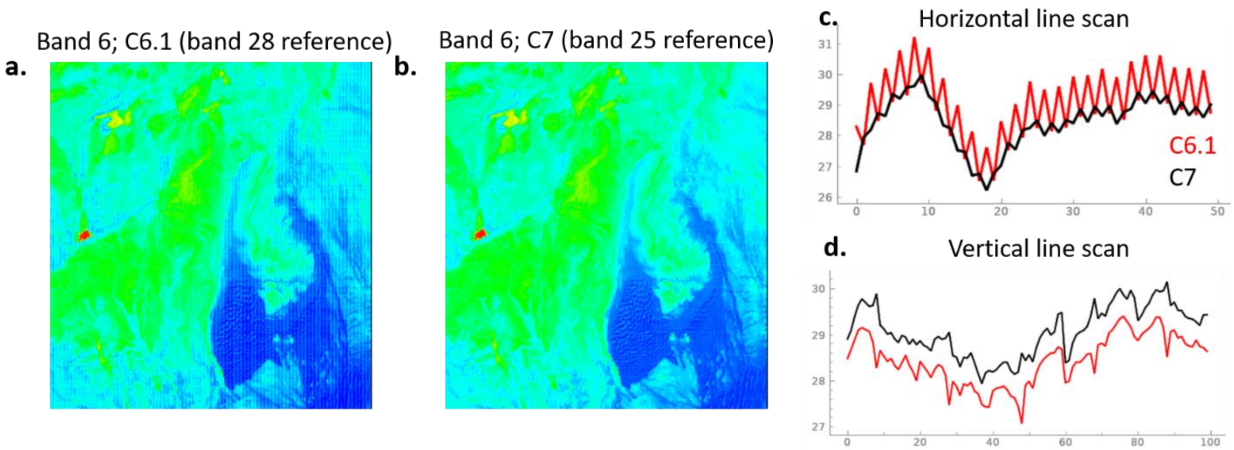

Figure 14. Earth view image at 500 m resolution from April 7, 2016 (granule 2016098.1055) for Terra band 6 using (a) C6.1 and (b) C7.[18] (c) A horizontal line scan through a portion of the image showing significant reduction in subframe (along-scan) striping in C7. (d) A vertical line scan through a portion of the image showing reduction in detector (along-track) striping in C7.

Another image quality improvement for C7, resulting from the combination of the use of polarization-corrected data and the RVS fitting enhancements, is a reduction in the mirror side striping in L1B reflectance for Terra bands 3, 8, and 9. In C6.1 L1B, for certain times in the mission, there were noticeable mirror side differences in the reflectance of up to a few percent. These arose from calibration errors in the fitting of the desert data (uncorrected for polarization). Figure 15 shows a comparison of the mirror side reflectance ratio for C6.1 compared to C7 for Terra band 8 observations from the Libya 4 desert site near nadir. Our new approach effectively eliminates the mirror side striping in the L1B. In C6.1, even though Fig. 15 shows that there is clearly mirror side striping of a few percent, the downstream C6.1 products should not be significantly affected by this error due to the polarization and de-trending corrections applied to the Level 2 products.

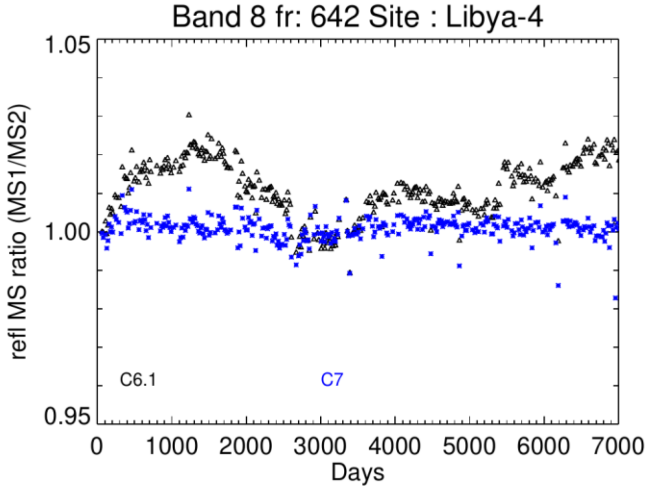

Figure 15. Ratio of reflectance from mirror side 1 to mirror side 2 over the mission (days since January 1, 2000) for Terra band 8 near nadir. Data are from observations of the Libya 4 desert site around frame 642 using the C6.1 (black) and C7 (blue) calibration algorithms. For both curves in this plot, the Libya 4 dn are corrected to remove polarization impact, and the only difference is the m_1/RVS LUTs used to evaluate the reflectance.

The change to use detector-dependent RVS for Terra band 4 also reduces the striping in the L1B reflectance. We evaluate this using DCC reflectance. Figure 16 shows the DCC reflectance detector differences for C7 before (a and c) and after (b and d) applying the detector-dependent RVS algorithm for this band. Clearly, the detector differences are smaller and more stable over the mission as a result of adding the detector dependence to the RVS. Lastly, the improved VF implemented in C7 for the Aqua ocean color bands causes a slight (within 1%) change in striping in the L1B reflectance for bands 13-16.

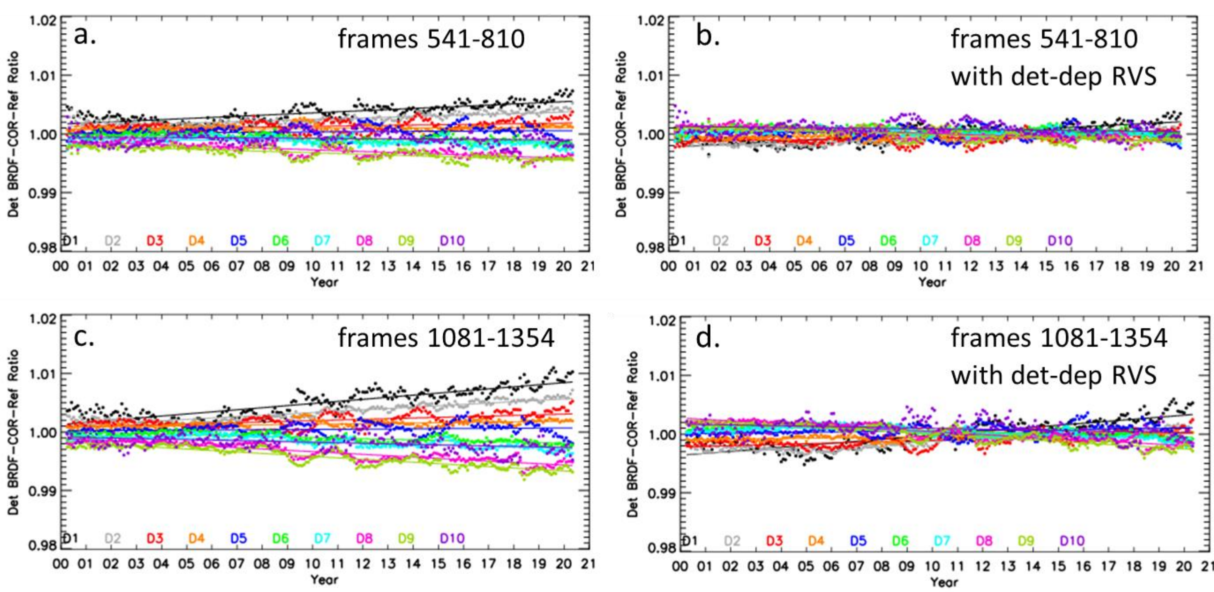

Figure 16. DCC reflectance detector differences—reflectance of each detector divided by the band average reflectance—for Terra band 4 for (a) near-nadir frame zone without detector-dependent RVS, (b) near nadir frame zone with detector-dependent RVS applied, (c) end-of-scan frame zone without detector-dependent RVS, and (d) end-of-scan frame zone with detector-dependent RVS applied. Different colors represent different 1-km aggregated detectors in L1B product order.

5. UNCERTAINTY UPDATES

The algorithm for deriving the L1B reflectance uncertainty, uncertainty LUTs, and L1B uncertainty index for C7 is mostly the same as that used in C6/C6.1, but with some necessary updates to account for some of the algorithm changes discussed in Section 3. The updates are only relevant for the bands that use Earth view data in deriving the calibration: Aqua bands 1-4 and 8-9, and Terra bands 1-12 and 26. All other bands use the same algorithm as is currently used in C6.1. Like the m_1 and RVS LUTs, all uncertainty LUTs used in generating the L1B uncertainty index have been regenerated for C7 using consistent reprocessed inputs, resulting in a smoother trend of uncertainty values over the mission compared to delivered C6.1 values.

The algorithm for C6/C6.1 RSB reflectance uncertainty has been presented in detail before[7]. The component of uncertainty due to the use of desert data in deriving adjustments to the on-orbit m_1 and RVS change is determined by estimating the uncertainty in the fitting of the desert data. The fitting of the desert data in C6.1 is done in two steps: an initial fitting of the trend at each frame over time, and then a fitting of the resulting smooth time curves over frame at each point in time to derive the final calibration. The standard deviations of the two sets of fitting residuals are calculated for each calendar year of the mission and the two are combined to get the EV fitting uncertainty component. The EV fitting component is then combined with the uncertainties from all other components to get the final uncertainty for each pixel. For C7, the desert data is processed in a slightly different way, and EV data from both ocean and DCC have been added to the algorithm for select Terra MODIS bands.

As presented in Section 3.2, the desert data for both Aqua and Terra MODIS are fit first over frame in C7, and then fit over time. A final fit over frame is done to get the LUT coefficients. To calculate the uncertainty in the fitting, the same strategy is used except there are now three sets of fitting residuals to combine to get the EV component of uncertainty. Practically, the residuals of the final frame fitting are small, and the total uncertainty is close in magnitude to that from the previous C6.1 fitting strategy. The desert data for bands 3, 8-10 of Terra MODIS are corrected for polarization prior to their use in deriving the calibration of these bands. The polarization correction is applied to individual desert observations and is independent of the strategy used for fitting the data, so no explicit change to the uncertainty algorithm is made due to the polarization correction.

For Terra bands 11 and 12, trends of ocean reflectance are generated using a ratio approach with band 4 as the reference band (Section 3.5). The ocean reflectance trends are fit first in time and then frame. The standard deviation of the two sets of fitting residuals are combined to get the uncertainty of the fitting of the on-orbit ocean reflectance trends. However, since the ocean data are referenced to band 4, the uncertainty in the fitting of the on-orbit trends of band 4 needs to be added. So the total EV component of the uncertainty for Terra bands 11 and 12 is the combined uncertainty of the fitting of bands 11 and 12 ocean reflectance data combined with the combined uncertainty of the fitting of band 4 desert reflectance data. Due to the effectiveness of the interband ratio, the ocean reflectance trends have fairly low noise, so in practice the uncertainty in bands 11 and 12 is only slightly larger than the uncertainty for band 4.

For Terra bands 5-7 and 26, the DCC reflectance trends are fit first over time and then over frame (Figures 6 and 7). Similar to the cases already discussed, the EV component to the uncertainty is the combination of the standard deviation of the fitting residuals from these fits. For the case of bands 5 and 26, the uncertainty varies as a function of frame and time to account for the overall uncertainty in m_1/RVS. For bands 6 and 7, there is no on-orbit RVS change, so the uncertainty is taken to be the same across all frames, based on the calculated value near nadir. Overall, the uncertainty for Terra SWIR bands in C7 is stable over time and slightly higher than the C6.1 uncertainty due to the added uncertainty in fitting the DCC data.

Figure 17 shows the total reflectance uncertainty for each Terra MODIS RSB at nadir and at typical radiance for a few years during the mission. The total reflectance uncertainty includes the EV data fitting uncertainty just described, as well as the uncertainties from pre-launch and on-orbit SD characterization, lunar observations, and the pixel-level signal noise evaluated at the typical radiance level for each band. Both C6.1 and C7 values are shown for comparison. For most bands there are no major changes. For bands 5, 6, 7, 11, 12, and 26, there are slight increases in the values for C7 due to the addition of EV data to the algorithm. For bands 3, 8-10, the C7 uncertainty is similar to C6.1 at nadir (shown in Fig. 17), but is significantly lower than C6.1 for frames near the edge of scan due to the reduction in noise of desert data after polarization correction.[12] Figure 18 shows the same reflectance uncertainty plots for Aqua MODIS C6.1 and C7. For Aqua, there are no meaningful changes in uncertainty values for C7. In both Figs. 17 and 18, the red line at 2% indicates the specified uncertainty requirement for MODIS RSB, with most bands remaining at or below this level throughout the missions for both instruments. While some Terra RSB have higher uncertainty values in C7, this should not be interpreted as a decrease in the quality of calibration. Rather, the calculation of the calibration uncertainty is being done more accurately in the C7 L1B to accompany a more accurate gain calibration and corrects biases that existed in C6.1 but were not accounted for in the C6.1 uncertainty.

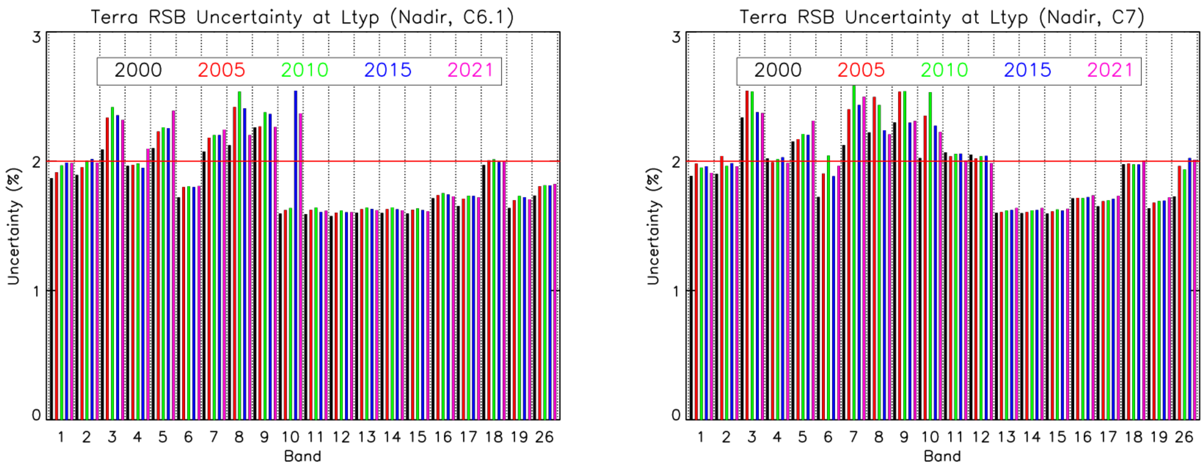

Figure 17. Reflectance uncertainty for each Terra MODIS RSB (averaged over all detectors, subframes and mirror sides within a band) at nadir and at typical radiance for a few years during the mission for (left) C6.1 and (right) C7.

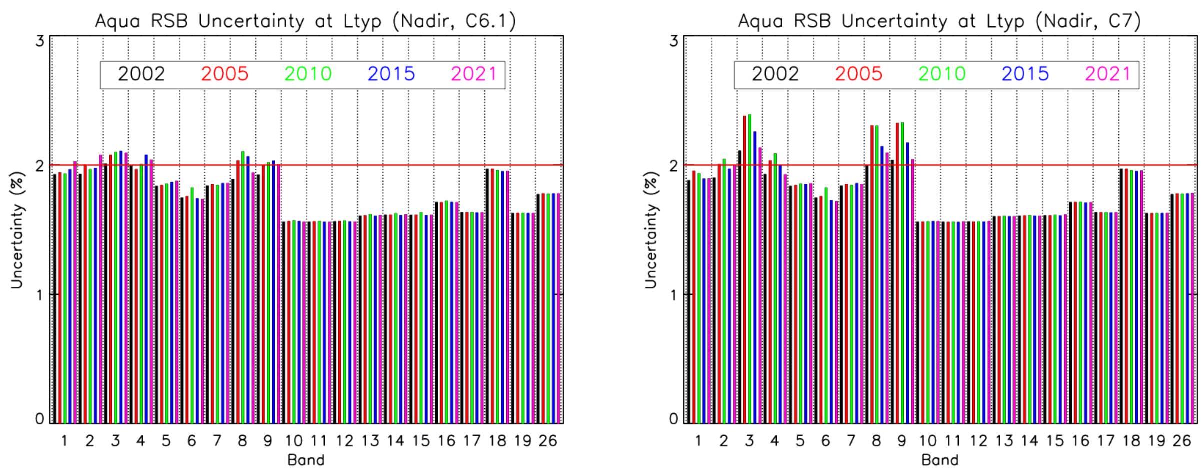

Figure 18. Reflectance uncertainty for each Aqua MODIS RSB (averaged over all detectors, subframes and mirror sides within a band) for a few years during the mission for (left) C6.1 and (right) C7.

6. SUMMARY

We have reviewed the RSB algorithm changes in Collection 7 L1B LUTs, relative to the algorithms used for the Collection 6.1 L1B LUTs. A majority of the discussed algorithm changes apply only to Terra MODIS, with relatively large changes of several percent seen for the short wavelength bands 3, 8-12, and SWIR bands. Aqua MODIS largely retains the C6.1 calibration strategies and there will be relatively small (<1% in nearly all cases) differences between the C6.1 and C7 L1B products. Overall, the C7 RSB reflectance and radiance products will provide a more accurate and stable calibration over the entire MODIS missions. This paper documents the final calibration algorithms that were used to deliver the C7 calibration LUTs for science testing in March and July 2021. MCST will update the C7 LUTs regularly and provide them as necessary for testing purposes, and will begin updating the LUTs in forward mode once official C7 L1B production begins. MCST will also work to maintain and improve MODIS RSB calibration going forward. Importantly, several different strategies are currently being explored to enable calibration of the MODIS instruments after the constellation exit maneuvers and extend the useful lifetime of MODIS data as far into the future as possible.

ACKNOWLEDGEMENTS

We thank other members of the MODIS Characterization Support Team for their efforts in developing and improving the RSB algorithms over the past 20+ years. We are especially grateful to Brent McBride for his help organizing the initial delivery of Collection 7 mission-reprocessed LUTs.

REFERENCES

[1] Barnes, W. L. and Salomonson, V. V., “MODIS: a global imaging spectroradiometer for the Earth Observing System,” Proc. SPIE **10269**, 102690G (1992).

[2] Xiong, X., K Chiang, J Esposito, B Guenther, and W Barnes., “MODIS on-orbit calibration and characterization,” Metrologia **40**(1), S89–S92 (2003).

[3] Sun, J., Xiong, X., Angal, A., Chen, H., Wu, A. and Geng, X., “Time-Dependent Response Versus Scan Angle for MODIS Reflective Solar Bands,” IEEE Trans. Geosci. Remote Sens. **52**(6), 3159–3174 (2014).

[4] Toller, G., Xiong, X., Sun, J., Wenny, B. N., Geng, X., Kuyper, J., Angal, A., Chen, H., Madhavan, S. and Wu, A., “Terra and Aqua moderate-resolution imaging spectroradiometer collection 6 level 1B algorithm,” J. Appl. Remote Sens. **7**(1), 073557 (2013).

[5] Xiong, X., Angal, A., Twedt, K. A., Chen, H., Link, D., Geng, X., Aldoretta, E. and Mu, Q., “MODIS Reflective Solar Bands On-Orbit Calibration and Performance,” IEEE Trans. Geosci. Remote Sens. **57**(9), 6355–6371 (2019).

[6] Bhatt, R., Doelling, D. R., Angal, A., Xiong, X., Haney, C., Scarino, B. R., Wu, A. and Gopalan, A., “Response Versus Scan-Angle Assessment of MODIS Reflective Solar Bands in Collection 6.1 Calibration,” IEEE Trans. Geosci. Remote Sens. **58**(4), 2276–2289 (2020).

[7] Xiong, X., Angal, A., Barnes, W. L., Chen, H., Chiang, V., Geng, X., Li, Y., Twedt, K., Wang, Z., Wilson, T. and Wu, A., “Updates of Moderate Resolution Imaging Spectroradiometer on-orbit calibration uncertainty assessments,” J. Appl. Remote Sens. **12**(03), 1 (2018).

[8] Aldoretta, E. J., Angal, A., Twedt, K. A., Chen, H., Li, Y., Link, D. O., Mu, Q., Vermeesch, K. and Xiong, X., “The MODIS RSB calibration and look-up table delivery process for collections 6 and 6.1,” Proc. SPIE **11501**, 115011Q (2020).

[9] Jun-Qiang Sun and Xiaoxiong Xiong., “MODIS Polarization-Sensitivity Analysis,” IEEE Trans. Geosci. Remote Sens. **45**(9), 2875–2885 (2007).

[10] Kwiatkowska, E. J., Franz, B. A., Meister, G., McClain, C. R. and Xiong, X., “Cross calibration of ocean-color bands from Moderate Resolution Imaging Spectroradiometer on Terra platform,” Appl. Opt. **47**(36), 6796 (2008).

[11] Meister, G., Eplee, R. E. and Franz, B. A., “Corrections to MODIS Terra calibration and polarization trending derived from ocean color products,” Proc. SPIE **9218**, 92180V (2014).

[12] Angal, A., Geng, X., Xiong, X., Twedt, K. A., Wu, A., Link, D. O. and Aldoretta, E., “On-Orbit Calibration of Terra MODIS VIS Bands Using Polarization-Corrected Desert Observations,” IEEE Trans. Geosci. Remote Sens. **58**(8), 5428–5439 (2020).

[13] Chen, H., Xiong, X., Angal, A., Geng, X. and Wu, A., “Alternative method of on-orbit response-versus-scan-angle characterization for MODIS reflective solar bands,” J. Appl. Remote Sens. **10**(2), 024004 (2016).

[14] Chen, H., Twedt, K., Vermeesch, K., Aldoretta, E., Angal, A. and Xiong, X., “MODIS Reflective Solar Band Calibration Improvements using Pseudo-Invariant Desert Targets,” Proc. SPIE **11829**, 118290Z (2021).

[15] Xiong, X., Chiang, K.-F., Adimi, F., Li, W., Yatagai, H. and Barnes, W. L., “MODIS correction algorithm for out-of-band response in the short-wave IR bands,” Proc. SPIE **5234**, 605 (2004).

[16] Moeller, C. C., Revercomb, H. E., Ackerman, S. A., Menzel, W. P. and Knuteson, R. O., “Evaluation of MODIS thermal IR band L1B radiances during SAFARI 2000,” J. Geophys. Res. Atmospheres **108**(D13), 8494 (2003).

[17] Wilson, T., Wu, A., Shrestha, A., Geng, X., Wang, Z., Moeller, C., Frey, R. and Xiong, X., “Development and Implementation of an Electronic Crosstalk Correction for Bands 27–30 in Terra MODIS Collection 6,” Remote Sens. **9**(6), 569 (2017).

[18] Xiong, X., Angal, A., Li, Y. and Twedt, K., “Improvements of on-orbit characterization of Terra MODIS short-wave infrared spectral bands out-of-band responses,” J. Appl. Remote Sens. **14**(4), 047503 (2020).

[19] Doelling, D. R., Morstad, D., Scarino, B. R., Bhatt, R. and Gopalan, A., "The Characterization of Deep Convective Clouds as an Invariant Calibration Target and as a Visible Calibration Technique," IEEE Trans. Geosci. Remote Sens. **51**(3), 1147–1159 (2013).
[20] Angal, A., Xiong, X., Mu, Q., Doelling, D. R., Bhatt, R. and Wu, A., "Results From the Deep Convective Clouds-Based Response Versus Scan-Angle Characterization for the MODIS Reflective Solar Bands," IEEE Trans. Geosci. Remote Sens. **56**(2), 1115–1128 (2018).
[21] Wilson, T. M., Aldoretta, E., Angal, A., Geng, X., Twedt, K. and Xiong, X., "Analysis of the on-orbit response-versus-scan-angle for the MODIS SWIR bands derived from lunar observations," Proc. SPIE **11530**, 115301E (2020).
[22] Geng, X., Angal, A., Li, Y., Twedt, K. A. and Xiong, X., "Improvements in the on-orbit response versus scan-angle characterization for the MODIS ocean color bands," Proc. SPIE **11151**, 1115124 (2019).
[23] Wang, Z. and Xiong, X., "Band-to-Band Misregistration of the Images of MODIS Onboard Calibrators and Its Impact on Calibration," IEEE Trans. Geosci. Remote Sens. **55**(4), 2136–2143 (2017).
[24] Mu, Q., Angal, A., Twedt, K., Wu, A. and Xiong, X., "MODIS detector differences using deep convective clouds and desert targets," Proc. SPIE **11530**, 115301A, SPIE (2020).
[25] Sun, J.-Q., Xiong, X., Barnes, W. L. and Guenther, B., "MODIS Reflective Solar Bands On-Orbit Lunar Calibration," IEEE Trans. Geosci. Remote Sens. **45**(7), 2383–2393 (2007).